http://dx.doi.org/10.21577/0100-4042.20170864 *Quim. Nova,* Vol. 45, No. 6, 654-658, 2022

Artigo

AMORPHOUS $CUSEP_2$/GRAPHENE COMPOSITES AS ANODE MATERIAL FOR ADVANCED POTASSIUM-ION BATTERY

Yu Luo[a,*], Qing Liu[a], Lingxiao Yang[a] and Youwei Yan[a#]
[a]State Key Laboratory of Material Processing and Die & Mould Technology, School of Materials Science and Engineering, Huazhong University of Science and Technology, Wuhan, Hubei 430074, China

Recebido em 14/08/2021; aceito em 14/12/2021; publicado na web em 16/02/2022

The ternary amorphous $CuSeP_2$ was designed and prepared as the anode material of potassium ion battery for the first time, and its electrochemical performance was also investigated. After ball-milling with commercial graphene powder, it is used as the anode material for potassium ion battery with reversible specific capacity up to 300 mAh g^{-1}, and the corresponding initial coulombic efficiency is close to 60%. What's more, the specific capacity remains above 150 mAh g^{-1} after 100 cycles at 200 mA g^{-1}. When increasing the current density to 1000 mA g^{-1}, the $CuSeP_2$/graphene composites still has a potassium storage specific capacity of 100 mAh g^{-1}. Our results show that the potassium storage mechanism of the ternary $CuSeP_2$ anode material is a typical conversion reaction and the introduction of Cu can not only buffer the volume expansion during the subsequent electrochemical reaction, but also effectively enhance the electrochemical reversibility of potassium ion.

Keywords: ball mill; potassium-ion battery; graphene; material; CuSeP2.

INTRODUCTION

Lithium-ion (Li-ion) batteries with high voltage, large capacity as well as stable cycling performance when compared with other energy storage devices such as lead-acid battery, nickel-metal hydride battery have achieved tremendous commercial success on some small energy storage devices such as the batteries of 3C products1. However, the scarcity and rising cost of Li sources restrict the application of Li-ion batteries in the large scale energy storage devices (e.g. the batteries of electric vehicles). It is essential to develop the alternatives of lithium-ion batteries.[1-3] Potassium-ion battery (K-ion battery) with rich abundance and low cost of K sources, has the potential to get rid of Li-ion battery.[4-6] Compared with sodium-ion battery, another possible alternative of Li-ion battery, K-ion battery holds the advantage of the lower redox potential of K (−2.93 V vs RHE) in contrast to Na (−2.7 V vs RHE), which is very close to that of Li element (−3.04 V vs RHE). So the K-ion battery would be a promising candidate for the next generation energy storage device. Unfortunately, the larger ionic radii of K+ (1.38Å) results in much slower electrochemical kinetics and poorer stability of the anode of potassium-ion battery compared with that of Li-ion battery.[7,8] To solve those drawbacks, various attempts have been made. Wang *et al.* first reported the potassium storage performance of graphite in carbonate electrolytes.[9] According to their research, the reversible specific capacity of the graphite anode is as high as 273 mAh g^{-1} at a current density of 1 C (279 mA g^{-1}). However, in the subsequent cycle, the specific capacity falls to 200 mAh g^{-1}, and even gradually decay to 80 mAh g^{-1} after 20 cycles. This is mainly due to the large ionic radius of potassium ions, which causes severe volume expansion of graphite upon K+ insertion. 2d structure material MXene had been research at other areas for many years and had made great progress.[10] Bao *et al.* have studied the Ti_3C_2 MXene as anode for potassium ion battery. A reversible specific capacity of 151 mAh g^{-1} at 50 mA g^{-1} can be obtained,[11] but the rate performance and initial coulombic efficiency are unsatisfactory.

Compared with carbon and metal carbides, metal phosphides with low cost, high capacity and high electric conductivity have drawn tremendous attention on the study of K-ion battery. Guo *et al.* reported the P-based Sn_4P_3/C composite as anode for potassium ion batteries.[12] The initial reversible specific capacity is as high as 384.8 mAh g^{-1}. However, the specific capacity decays rapidly to 0 mAh g^{-1} after 35 cycles. Even after carbon coating, the final cycle performance is still poor. Considering the high capacity and low-cost of P-based material,[13] in this work, we designed a ternary amorphous $CuSeP_2$ compound. After balling with commercial graphene, a novel anode material ($CuSeP_2$/graphene) with high initial coulomb efficiency, good rate performance and long cycling life can be obtained for potassium ion battery. To the best of our knowledge, it is the first time for this material employed in potassium ion battery research.[14-16]

EXPERIMENTAL

Chemicals

Copper powder (AR), Selenium powder (99.9%, metals basis), Red Phosphorus powder (AR, 98.5%), Copper acetate monohydrate (AR, 99.0%) ,Graphene powder (Diameter: 8*8 μm* μm Purity:99%), Aqueous graphene oxide dispersion (Reagent grade, 1mg/mL) were purchased from Aladdin company.

Materials synthesis

Synthesis of $CuSeP_2$

The amorphous $CuSeP_2$ compound was prepared by a simple ball milling method. Typically, the stoichiometric ratio of Cu powder, Se powder and red phosphorus are sealed in an 80 ml ball mill jar under an argon atmosphere with tungsten carbide grinding balls inside. The ball-to-powder weight ratio was fixed at 30/1.[17,18] The ball-milling process was perform on the MSK-SFM-1 ball mill grinder. After mechanical milling for 20 hours at an optimized rotating frequency of 20 Hz, the synthesized $CuSeP_2$ sample was harvested.

*e-mail: 416838455@qq.com
#alternative e-mail: yanyw@hust.edu.cn

Synthesis of $CuSeP_2$-G

a certain amount of prepared $CuSeP_2$ sample and 5% graphene powder were mixed in the same ball mill jar. The mass ratio of ball-to-powder was fixed at 20:1. After 2 hour of ball milling, the $CuSeP_2$/Graphene composites were obtained.

Synthesis of nano-Cu/r-Graphene/P

The composite of nano-Cu particles anchored on graphene was also prepared.[19] Firstly, a certain amount of copper acetate monohydrate is dissolved in the aqueous graphene oxide dispersion, and then was frozen dried for 48 hours. Finally, the freeze-dried sample is subjected to high temperature treatment in an argon/ydrogen atmosphere (5% H2: 95% Ar v/v) for 6 hours under 400 °C.[20,21] Then the obtained product was mixed with the ball-milled red phosphorus in a mortar by hand to form nano-Cu/r-Graphene/P composite.

Synthesis of CuSe-G, CuP_2-G, Se-P-G

The above mentioned binary composite compound was prepared by the same ball mill process like $CuSeP_2$ but not the specific third element powder to add in, and then same method to ball mill with the graphene powder.

Characterizations

The XRD pattern was tested on an X'pert PRO MRD diffractometer with Cu Kα radiation from 10° to 80°. The Scanning electron microscopy (SEM) images and the EDX analysis of the single-particle samples was conducted on FEI Nova NanoSEM 450 field emission scanning electron microscope equipped with an Oxford energy spectrum probe and an energy spectrum analysis technique. The Transmission electron microscopy (TEM) images and elected electron diffraction (SAED) test were performed using Tecnai G2 F30 field emission transmission electron microscope.

Electrochemical measurements

The slurry was mixed in a mass ratio of 80% active material (to the pure carbon sample, the electrode the active materials is Super-P), 10% Super-P carbon black, and 10% PAA-Na. After homogeneous mixing, the slurry was casted onto copper foil and transferred to an oven at 80 °C for drying, which was then cut into 8 mm wafers. The loading mass of the active material is substantially 1.5-3 mg/cm^2. The counter electrode used in the assembly of the potassium ion battery is potassium. Since the potassium is too active, all operations must be performed in a high purity argon glove box. The electrolyte used in the assembly of the potassium ion battery was a self-made 0.8 mol L^{-1} KPF6/ diethyl carbonate / ethylene carbonate electrolyte, the carbonate ratio for the electrolyte was 1:1 vol. In addition, Whatman glass fiber membrane was utilized as separator.

RESULTS AND DISCUSSION

Figure 1(a) and Figure 1S shows the XRD patterns of the prepared $CuSeP_2$ samples. For comparison, we also prepared Se-P, CuSe, CuP_2, Cu, P and Se samples by ball milling. It can be seen that after 26 hours of ball milling, the $CuSeP_2$ sample exhibited broad diffraction peaks, relate to the transmission electron microscopy images(Figure 1b, 1c, 1d), these indicates the structure of the material is amorphous.[22,23] At the same time, we can see that Se-P has also been amorphization after ball milling, which may be due to the formation of Se-P amorphous compounds in the product, as reported by other researchers.[24] However, after the same ball milling treatment, the samples of CuSe, CuP_2, Se, Cu and P still exhibit strong crystallinity.

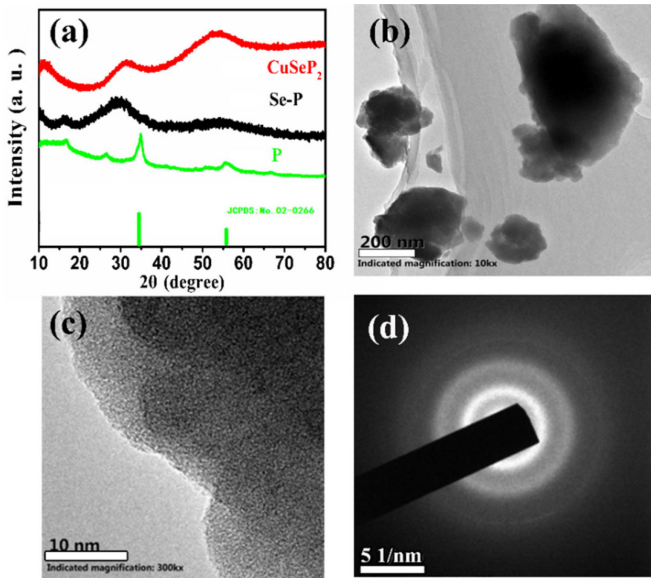

Figure 1. *(a) XRD patterns of $CuSeP_2$, Se-P, P samples after ball-milling (b) TEM, (c) HRTEM and (d) SAED images of the $CuSeP_2$ sample*

The microstructure of the synthesized $CuSeP_2$ was also further studied. The obtained TEM images and selected electron diffraction (SAED) are shown in Figure 1b, 1c, 1d. It can be seen that the particle size of prepared $CuSeP_2$ samples is nano-scale. Large particles are mainly agglomerated by nano-sized particles. The high-resolution transmission images does not show any lattice fringes, and the selected area electron diffraction pattern shows that all of the particles exhibit diffraction rings. It was further proved that the $CuSeP_2$ sample had an amorphous structure. The SEM images of $CuSeP_2$ samples and $CuSeP_2$/graphene composites are shown in Figure 2.

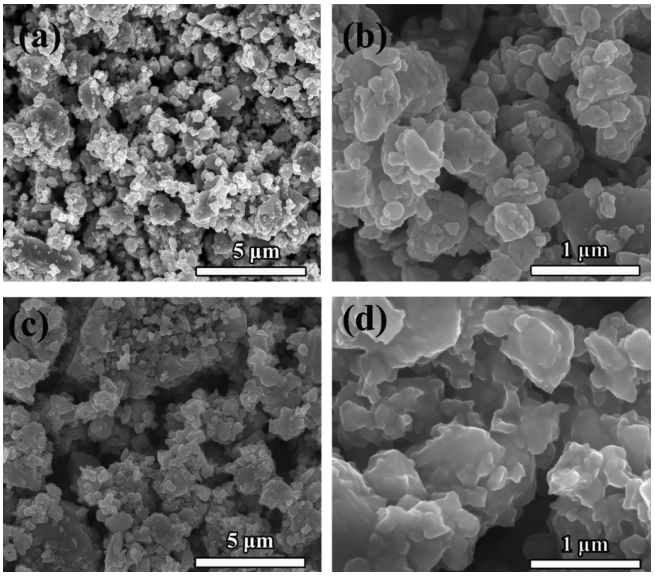

Figure 2. *The SEM images of $CuSeP_2$ sample (a, b) and $CuSeP_2$/graphene composite (c, d)*

It can be seen from the images that the particles exhibit an irregular shape, which is agglomerated. In order to investigate the elemental ratio, we performed EDX analysis on the sample (Figure 2S). It can be seen from the EDX spectrum analysis (Table 1S) that the atomic percentages of Cu, Se and P are very close to 1:1:2, which is basically consistent with the theoretical stoichiometric

ratio. EDX analysis was also performed on single particle to confirm element distribution information (Figure 3S).

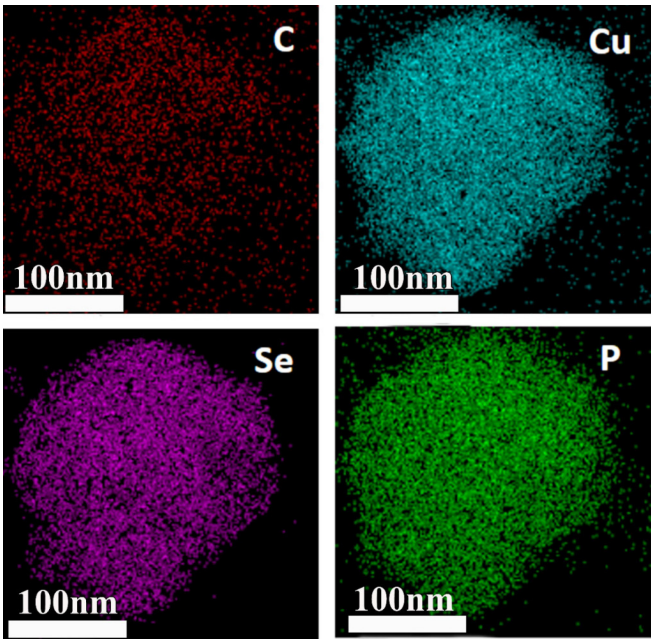

Figure 3. *EDX analysis of single $CuSeP_2$ particles after graphene coating*

Figure 3S also shows the uniform distribution of Cu, Se, P elements and no other impurity is detected, further indicating the purity of $CuSeP_2$ sample. In addition, elemental distribution analysis on graphene-coated samples (Figure 3) indicates that carbon element reveal on the particles after ball milling. Graphene can not only provide more electron conduction channels and accelerate the electrochemical reaction, but also prevent the rapid decay of capacity caused by particle pulverization.[25,26]

The electrochemical performance of the $CuSeP_2$/Graphene samples was further investigated, the pure carbon sample was set as control sample. As shown in Figure 4(a), the first discharge capacity of the $CuSeP_2$/Graphene electrode material delivered high specific capacity of 500 mAh g^{-1} at 50 mA g^{-1} and the reversible specific capacity was more than 300 mAh g^{-1}, corresponding to an initial coulombic efficiency of about 60%. And the pure carbon sample delivered a specific capacity of 274 mAh g^{-1} at 50 mA g^{-1} and the reversible specific capacity was more than 131 mAh g^{-1}, corresponding to the initial coulombic efficiency of about 47%. The larger size ionic radius of potassium ions leads to more sluggish electrochemical kinetics, which often causes high irreversible capacity of the anode material and low coulomb efficiency.[27] In addition, the specific capacity remains above 150 mAh g^{-1} after 100 cycles at 200 mA g^{-1}, except for a slight decrease in the first few cycles, showing excellent electrochemical stability of $CuSeP_2$/Graphene (Figure 4b). The control sample only remains the specific capacity about 40 mAh g^{-1} after 100 cycles at 200 mA g^{-1}. Rate performance (Figure 4c) was measured with current density of 200, 500, 1000 mA g^{-1} while the $CuSeP_2$/Graphene anode materials can maintain capacities of 200, 150 and 100 mAh g^{-1}, respectively. The sample pure carbon only deliver a capacities of 85 mAh g^{-1} at 200 mA g^{-1} and fade to almost zero at a higher current density (Figure 4c). When reducing the current density from 1000 mA g^{-1} to 50 mA g^{-1}, the specific capacity can be quickly recovered to 280 mAh g^{-1}. The above results shows that the $CuSeP_2$/Graphene anode material has excellent rate performance in potassium ion batteries.

We conducted *ex situ* TEM observations on $CuSeP_2$ anode material with different charge and discharge depths to figure out its potassium ion storage mechanism. As shown in Figure 5a and 5b, when discharged to 0.001 V, most of the micron-sized $CuSeP_2$ particles have been pulverization. At the same time, lattice fringes corresponding to K_3P and K_2Se were clearly observed, corresponding to their (110) and (220) planes, respectively. Interlayer spacing of 0.209 nm is assigned to (111) plane of nano-copper.

When recharged back to 2 V, as shown in Figure 5c and 5d, no apparent crystal particles are observed and the whole sample exhibits amorphous state. Thus, we can infer that the electrochemical reaction of the ternary $CuSeP_2$ anode material in potassium ion storage is a typical conversion reaction.

For comparison, the electrochemical performance of single phase graphene-coated P, Se, Cu, as shown in the Figure 4S. It can be seen that the first reversible specific capacity of P/graphene composite and Se/graphene composite is still very low, and the nano-Cu/graphene composite is electrochemical inertia. The inset in the Figure 4S show the cycle electrochemical performance of the above samples, the specific capacity of those single phase samples dramatic decay to zero. The synergistic effects of multi-phases may play an important role in the $CuSeP_2$ composite for the electrochemical performance.

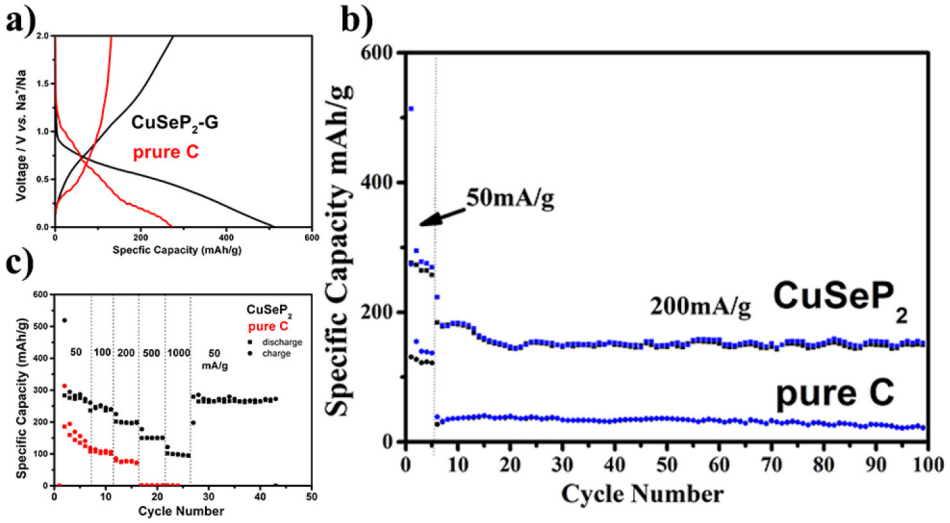

Figure 4. *The electrochemical performance of $CuSeP_2$/Graphene composite and the pure C: a) Discharge-charge curve between 0.001 V-2.0 V. b) Cycle performance. C) Rate performance*

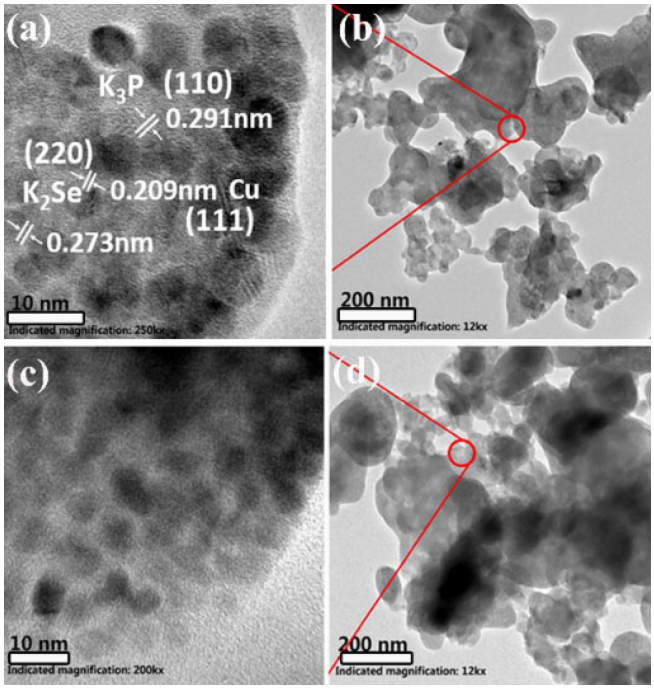

Figure 5. *(a) TEM and (b) HRTEM images of sample discharged to 0.001 V, (c) TEM and (d) HRTEM images of sample recharged to 2 V*

For further research, the electrochemical performance of the binary composite phases with graphene-coated samples detected. Cu-Se composite (stoichiometric ratio 2:1), Se-P composite (stoichiometric ratio 1:1), and CuP_2 was also investigated. The galvanostatic curves and cycle performance are shown in Figure 6. While the reversible charge capacities of Se-P/graphene and Cu-Se/graphene composites is relatively high, which suggests that the electrochemical activities of Se-P amorphous composites and Cu-Se composites are significantly improved, indicating that multi-element synergy may play an important role in the potassium ion storage. The CuP_2 sample exhibits reversible charge capacities about 100 mAh g^{-1}. The cycle electrochemical performance of the sample CuSe-G presented in the inset of Figure 6, show that Cu-Se/graphene also has superior cycling life, indicating that the introduction of Cu can also improve the cycle stability of Se. The nano-copper particles generated during the *in situ* electrochemical reaction can not only increase the electronic conductivity of the electrode, but also contribute to inhibiting the drastic volume change during charging/discharging process.[28] Many researcher had been study the synergistic effects of multi-phases materials battery.[29] In order to reveal the effect of nano-Cu on the electrochemical behavior, we prepared nano-Cu/r-Graphene, in which nano-copper particles are anchored on reduced oxide graphene, and mixed it with the ball-milled red phosphorus in a mortar by hand to form nano-Cu/r-Graphene/P composite. As anode material for potassium ion batteries, the initial reversible charge specific capacity of nano-Cu/r-Graphene/P is obviously increased to above 200 mAh g^{-1} (Figure 5S) when compared to P/graphene, showing that nano-copper particles have a significant catalytic effect on the electrochemical activity. Nano transition metals like copper can largely enhance the electrical conductivity of the electrodes owe to its excellent conductivity and electro catalytic activity. This phenomenon also reported by other literatures. The specific capacity rapidly decays to 0 mAh g^{-1} only after 4 cycles, mainly because of the poor coating contact of graphene and red phosphorus by manual mixing.[30,31] Figure 6S summarized the difference of this work and others work report for potassium-ion battery.[32-36]

CONCLUSIONS

We designed and prepared a ternary $CuSeP_2$/Graphene by a facile ball milling method and investigated its electrochemical performance as the anode material for advanced potassium ion battery for the first

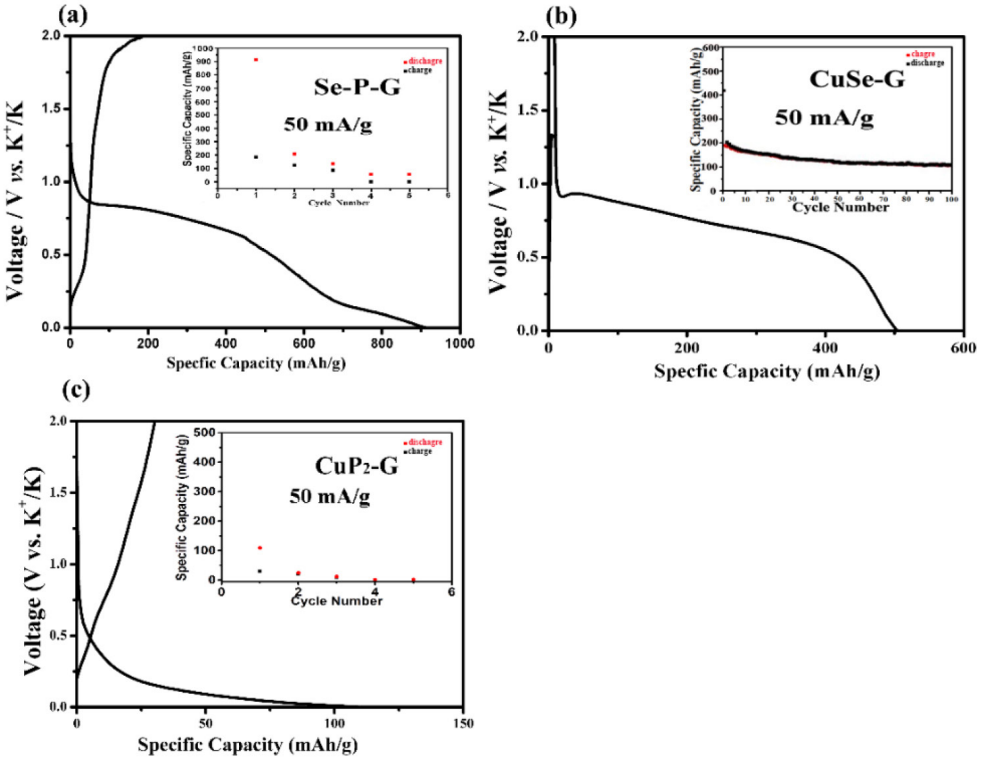

Figure 6. *The first discharge/charge curve of the binary composite phases with graphene-coated samples and the inset corresponds to the cycle electrochemical performance. (a) Se-P-G, (b) CuSe-G, (c) CuP_2-G*

time. At 50 mA g^{-1}, the $CuSeP_2$/Graphene delivers a reversible specific capacity of 300 mAh g^{-1}, corresponding to an initial coulombic efficiency of 60%. After 100 cycles, the specific capacity can remain above 150 mAh g^{-1} at 200 mA g^{-1}. When increasing the current density to 200, 500 and 1000 mA g^{-1}, the specific capacities of 200, 150 and 100 mAh g^{-1} can be maintained respectively. Our results show that $CuSeP_2$/Graphene exhibits superior cycling and rate ability in advanced potassium ion battery. The introduction of Cu plays an important role in improving the electrochemical activity of the P and Se elements, which may guide the material design and further development of potassium-ion battery in the future.

SUPPLEMENTARY MATERIAL

Figures 1S to 6S and Table 1S are available at http://quimicanova.sbq.org.br in pdf format, with free access.

ACKNOWLEDGEMENTS

This work was supported by the National Key R&D Program of China (2016YFB0100302), the Key Fundamental Research Project from Shenzhen Research Council (JCYJ20150616144425387), and the Natural Science Foundation of China (Grant No. 51002054 and 60306011). The authors also thank the State Key Laboratory of Materials Processing and Die & Mould Technology of HUST and the Analytical and Testing Centre of HUST for XRD, SEM and other measurements.

REFERENCES

1. Liu, H.; Li, C.; Zhang, H. P.; Fu, L. J.; Wu, Y. P.; Wu, H. Q.; *J Power Sources* **2006**, *159*, 717.
2. Wang, H. Y.; Ren, Y.; Wang, W. J.; Huang, X. B.; Huang, K. L.; Wang, Y.; Liu, S. Q.; *J Power Sources* **2012**, *199*, 315.
3. Xiong, S. L.; Chen, J. S.; Lou, X. W.; Zeng, H. C.; *Adv. Funct. Mater.* **2012**, *22*, 861.
4. Eftekhari, A.; Jian, Z. L.; Ji, X. L.; *ACS Appl. Mater. Interfaces* **2017**, *9*, 4404.
5. Zhao, Q.; Wang, J. B.; Lu, Y.; Li, Y. X.; Liang, G. X.; Chen, J.; *Angew. Chem., Int. Ed.* **2016**, *55*,12528.
6. Zou, X. X.; Xiong, P. X.; Zhao, J.; Hu, J. M.; Liu, Z. T.; Xu, Y. H.; *Phys. Chem. Chem. Phys.* **2017**, *19*, 26495.
7. Xu, Z. Q.; Wu, M. Q.; Chen, Z.; Chen, C.; Yang, J.; Feng, T. T.; Eunsu, P.; David, M.; *Advanced Science.* **2019**, *6*, 2272.
8. Kubota, K.; Dahbi, M.; Kumakura, S. T.; Komaba, S.; *Chem. Rec.* **2018**, *18*, 459.
9. Liu, Y.; Fan, F. F.; Wang, J. W.; Liu, Y.; Chen, H. L.; Jungjohann, K. L.; Xu, Y. X.; Zhu, Y. J.; Bigio, D.; Zhu, T.; Wang, C. S.; *Nano Lett.* **2014**, *6*, 3445.
10. Ameen, U. A.; Ipek, D. Y.; Feray, B.; Emre, E.; *Beilstein J. Nanotechnol.* **2021**, *12*, 49.
11. Dong, Y. F.; Wu, Z. S.; Zheng, S. H.; Wang, X. H.; Qin, J. Q.; Wang, S.; Shi, X. Y.; Bao, X. H.; *ACS Nano* **2017**, *5*, 4792.
12. Zhang, W. C.; Mao, J. F.; Li, S.; Chen, Z. X.; Guo, Z. P.; *J. Am. Chem. Soc.* **2017**, *9*, 3316.
13. Ortega, D.; Hernández-Garrido, J. C.; Blanco-Andujar, C.; Garitaonandia, J. S.; *J. Nanopart. Res.* **2013**, *15*, 2120.
14. Feng, Y. H.; Chen, S. H.; Shen, D. Y.; Zhou, J.; Lu, B. G.; *Energy Environ. Mater.* **2020**, *0*, 1.
15. Yang, H.; Xu, R.; Yao, Y.; Ye, S. F.; Zhou, X. F.; Yu, Y.; *Adv. Funct. Mater.* **2019**, *29*, 1809195.
16. Yu, S.; Kim, S. O.; Kim, H. S.; Choi, W. C.; *Int J Energy Res.* **2019**, *43*, 7646.
17. Zhang, T. R.; Jiang, X.; Li, G. C.; Yao, Q. F.; Lee, J. Y.; *ChemNanoMat* **2017**, *4*, 56.
18. Gao, Y. Q.; Ru, Q.; Liu, Y.; Cheng, S. K.; Wei, L.; Ling, F. C. C.; Chen, F.; Hou, X. H.; *ChemElectroChem* **2019**, *6*, 4689.
19. Wang, P.; Shen, M. Q.; Zhou, H.; Meng, C. F.; Yuan, A. H.; *Small* **2019**, *15*, 1903522.
20. Wang, B.; Zhang, C.; Wang, J. K.; An, H.; Guo, Z. M.; Lv, Z. G.; *Appl. Organomet. Chem.* **2019**, *33*, e5000.
21. Takeda, M.; Saeki, A.; Sakamoto, J. C.; Imai, Y.; Ichikawa, H.; *J. Am. Ceram. Soc.* **2000**, *83*, 1063.
22. Verdy, A.; Acapito, F.; Dory, J. B.; Navarro, G.; Bernard, M.; Noé, P.; *Phys. Status Solidi RRL* **2019**, *14*, 1900548.
23. Niu, X. G.; Zhang, Y. C.; Tan, L. L.; Yang, Z.; Yang, J.; Liu, T.; Zeng, L.; Zhu, Y. J.; Guo, L.; *Energy Storage Mater.* **2019**, *22*, 160.
24. Feldmann, K. O.; Wiegand, T.; Ren, J. J.; Weigand, J. J.; *Chem. – Eur. J.* **2015**, *21*, 9697.
25. Raccichini, R.; Varzi, A.; Wei, D.; Passerini, S.; *Adv. Mater.* **2017**, *29*, 160342.
26. Wang, R. H.; Liu, M. M.; Sun, J. In *Graphene-based Energy Devices*; Yusoff, A. R. B., ed.; Wiley-VCH: New York, 2015, p. 49.
27. Ding, Y.; Guo, X. L.; Qian, Y. M.; Zhang, L. V.; Xue, L. G.; Goodenough, J. B.; Yu, G. H.; *Adv. Mater.* **2019**, *31*, 1806956.
28. Li, X. L.; Li, M.; Yang, Q.; Liang, G. J.; Huang, Z. D.; Ma, L. T.; Wang, D. H.; Mo, F.; Dong, B. B.; Huang, Q.; Zhi, C. Y.; *Adv. Energy Mater.* **2020**, *10*, 2001791.
29. Zhang, Y. F.; Yang, J.; Zhang, Y. Z.; Li, C. C.; Dong, X. C.; *ACS Appl. Mater. Interfaces* **2018**, *10*, 12722.
30. Wang, K.; Huang, J. G.; *Appl. Surf. Sci.* **2019**, *476*, 293.
31. Poizot, P.; Laruelle, S.; Grugeon, S.; Dupont, L.; Tarascon, J. M.; *Nature* **2000**, *407*, 496.
32. Ma, H. L.; Qi, X. J.; Peng, D. Q.; Chen, Y. X.; Wei, D. H.; Ju, Z. C.; Zhuang, Q. C.; *ChemistrySelect* **2019**, *4*, 11488.
33. Chen, Z.; Chen, S. L.; Zhang, H. F.; Liu, M. Q.; Feng, Z. J.; Li, X. B.; Huang, J. T.; Guo, D.; *Ionics* **2020**, *26*, 1779.
34. Zhang, W. Z.; Wang, H. L.; Liao, R. X.; Wei, W. R.; Li, X. C.; Liu, S.; Huang, M. H.; Shi, Z. C.; Shi, J.; *New Carbon Mater.* **2021**, *36*, 167.
35. Huang, H. W.; Etogo, C. A.; Chen, C.; Bi, R.; Zhang, L.; *ACS Appl. Mater. Interfaces* **2021**, *13*, 36982.
36. Qi, S. H.; Xie, X.; Peng, X. W.; Ng, D. H. L.; Wu, M. G.; Liu, Q. H.; Yang, J. L.; Ma, J. M.; *Phys. Status Solidi RRL* **2019**, *13*, 1900209.